

STRUCTURAL AND OPTICAL CHARACTERIZATION OF MAGNETRON SPUTTERED ZnS THIN FILMS ANNEALED IN DIFFERENT ATMOSPHERE

L. KONG, J. DENG*, L. CHEN

College of Applied Sciences, Beijing University of Technology, Beijing, 100124, China

ZnS is an important wide band gap semiconductor with extensive potential applications. ZnS thin films were deposited on quartz glass substrates by radio frequency (RF) magnetron sputtering, and then were annealed at 200°C, 350°C and 500°C temperatures in a vacuum atmosphere and a sulfur atmosphere respectively. Effects of the different annealing atmosphere on structure, optical constants, Raman properties and band gap of the ZnS films were investigated. XRD data shows cubic structure for all the films with (111) as the highly preferential orientation, and shows that sulfur atmosphere is better to crystalline quality than vacuum. EDS analysis shows that the sulfur atmosphere can elevate S atomic percentage. Optical constants were obtained using ellipsometry analysis. Raman spectra also supports that the sulfur atmosphere is helpful to crystalline quality. The transmission spectra were measured and the band gap of 3.16 - 3.39eV was obtained using Tauc formula and extrapolation method. The band gap of the films annealed in S atmosphere has a blue shift compared with that annealed in vacuum at every same annealing temperature. It is demonstrated that ZnS films possessing good structural and optical properties can be obtained by the RF magnetron sputtering and the sulfur atmosphere annealing route.

(Received December 15, 2016; Accepted March 7, 2017)

Keywords: RF magnetron sputtering, ZnS thin films, Annealing, Vacuum atmosphere, Sulfur atmosphere

1. Introduction

Zinc sulfide (ZnS) is an important wide band gap semiconductor material with extensive potential applications, such as flat-panel displays, sensor, light-emitting diodes, photodetectors and solar cells [1-5]. In the important application of photovoltaics, ZnS can be used as buffer layer material of CuInGaSe₂ (CIGS), Cu₂ZnSnS₄ (CZTS) thin-film solar cells [6, 7]. Compared to CdS used commonly as buffer layer material, ZnS has some advantages: nontoxic, abundant, cheap, lattice matched with CIGS or CZTS absorber, possessing wide band gap. ZnS is a direct band gap n type semiconductor. The band gap of ZnS is in the range of 3.2 ~ 3.9 eV [8], while the band gap of CdS is only about 2.45eV [9]. The wide band gap of ZnS enables high energy incident photons to reach the window-absorber junction, enhancing the blue response of the photovoltaic cells and thus contributes to a better cell performance. The main fabrication methods of ZnS films involve chemical bath deposition [10], chemical vapor deposition [11], molecular beam epitaxy [12], thermal evaporation [13] and RF magnetron sputtering [14]. Among these fabrication methods, magnetron sputtering technique has some advantages such as easier controllability of the deposition parameters, high film growth rate, compatibility with the sputtering depositions of absorber and window layer and thus beneficial to industrial production of solar cells[15]. Thin film solar cells with high efficiency require thin films fabricated with high quality. Annealing is one method used often to improve film quality. In this work, ZnS thin films were deposited on quartz glass substrates by RF magnetron sputtering, and then were annealed in a vacuum atmosphere and

*Corresponding author: jdeng@bjut.edu.cn

a sulfur atmosphere respectively. The effects of different annealing atmosphere on structural and optical properties of ZnS films sputtered were studied comparatively.

2. Experimental details

ZnS films were deposited by RF magnetron sputtering system on quartz glass substrates. Quartz glass was adopted as substrate because of its transparency in the range of ultraviolet and visible which is convenient to measure transmittance spectrum and wide band gap of ZnS. The substrates were cleaned ultrasonically in acetone - ethyl alcohol - deionized water sequence, and then were dried by nitrogen gas flow before deposition. Source material is a 60 mm diameter water-cooled ZnS sputtering target (99.99%). The working pressure during the deposition procedure was kept at 1 Pa by flowing 25 sccm of purified argon (99.999%) as the working gas into the chamber. RF-sputtered ZnS films were grown with 100 W power in the absence of intentional substrate heating. The ZnS target was pre-sputtered for 15 minutes to avoid the film contamination induced by impurities on the target's surface. After RF-sputtering, the deposited ZnS films were annealed for 1 hour at 200°C, 350°C and 500°C temperatures in a vacuum atmosphere and a sulfur atmosphere respectively in a modified close equipment using one heater for vacuum annealing and using two heaters for S atmosphere annealing. The chamber was evacuated to 3×10^{-3} Pa initially. For S atmosphere annealing, the sulfur powder was mounted on a isolated heater. After annealing, the samples were kept in vacuum until cooled down. Structural and crystalline properties were examined by x-ray diffractometer (XRD; Pgeneral XD-3) with Cu K_{α} radiation wavelength, $\lambda = 1.54 \text{ \AA}$. The surface morphology and atomic ratio were observed by field-emission scanning electron microscopy (SEM-EDS; FEI QUANTA FEG 650) equipped with energy dispersive x-ray spectroscopy module. Optical constants (n, k) of the films were obtained using ellipsometer (Jobin Yvon MM-16) and DeltaPsi2 software. The Raman spectrum was obtained using a Raman spectrometer (JY T64000) with 514 nm incident laser beam. Optical transmission measurements were performed at room temperature by using UV/VIS/NIR spectrophotometer (Shimadzu UV3600). Energy band gap values were calculated from the obtained transmission spectra.

3. Results and discussion

3.1. XRD data and structural properties

Fig. 1 shows the XRD spectra of the ZnS films annealed in vacuum and S atmosphere respectively in the range from 20° to 60° at 200°C, 350°C and 500°C temperatures. All the films exhibit a strong peak at 28.6° and a weak peak [see partial enlargement figure in Fig. 1(a)] at 59.3° both corresponding to (111) plane of cubic structure of ZnS. The strong peak is the first order diffraction of (111) plane and the weak one is the second order diffraction of the same plane [Joint Committee on Powder Diffraction Standards (JCPDS) card 05-0566]. All the films even including the unannealed have obvious highly preferred orientation, which indicates that the RF magnetron sputtering method in this work are suitable to fabricate ZnS films. Whether for vacuum annealing or for S atmosphere annealing, after 200°C or 350°C annealing the intensity of (111) major diffraction peak of the films is strengthened, which means the crystallinity of the films is further improved, because annealing treatment can make atoms of the films be rearranged with increased kinetic energy and then make defects of the films reduced.

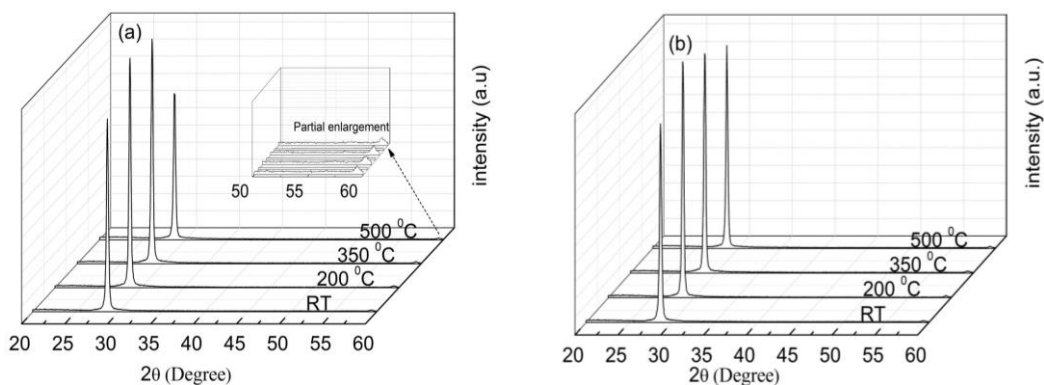


Fig. 1. XRD pattern of ZnS films annealed at 200°C, 350°C, 500°C in different atmosphere.

(a) Vacuum; (b) S atmosphere. "RT": unannealed.

When the annealing temperature reaches 500°C, the difference between vacuum annealing and S atmosphere annealing appears: for vacuum annealing the intensity of (111) major diffraction peak drops apparently, while for S atmosphere annealing that drops not so apparently. For 500°C vacuum annealing the major peak intensity drops for two reasons: one reason is that at higher temperature, the thermal stress increases resulting from the difference of thermal expansion coefficient between ZnS film and quartz substrate which influences the crystalline quality of ZnS film and even causes a few cracks visible to the naked eye. The other reason is the S reevaporation at higher temperature, leading to more S vacancy defects and the decline of crystalline quality. The ZnS film annealed at 500°C in S atmosphere is also affected by the thermal stress, but the S reevaporation can be restrained in S atmosphere, so the decline of crystalline quality is not as apparent as that of the film annealed at 500°C in vacuum.

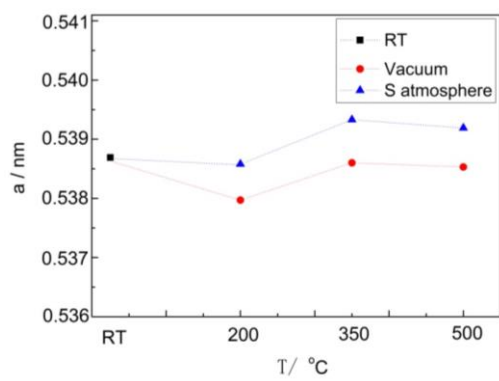


Fig. 2. The lattice constant of ZnS films annealed at 200°C, 350°C, 500°C in different atmosphere.

The crystalline interplanar spacing (d) of the samples was calculated using Bragg equation:

$$2d\sin\theta = n\lambda \quad (1)$$

where θ is diffraction angle, n is diffraction order, λ is wavelength of X ray ($\lambda = 0.154\text{nm}$; copper target), and all the d values calculated were about 0.311nm which is consistent with standard data of (111) interplanar spacing of cubic ZnS. Lattice constant (a) of cubic ZnS can be obtained by the equation:

$$a = d(h^2 + l^2 + k^2)^{1/2} \quad (2)$$

where h , l , and k are Miller indices. Mean grain size (D) can be evaluated using Scherrer equation:

$$D = 0.89\lambda/(\beta\cos\theta) \quad (3)$$

where β is the full-width at half-maximum (unit: rad). Lattice constant and mean grain size were calculated from the equations mentioned above according to the XRD data of (111) major diffraction peak. Contrast data of lattice constant for the ZnS films annealed in different atmosphere (vacuum or S atmosphere) are shown in Fig. 2. At every same temperature, the lattice constant of the film annealed in S atmosphere is always larger than that annealed in vacuum, closer to 5.4 \AA , which implies that the ZnS films annealed in S atmosphere could be more lattice matched with absorber layer if used as buffer layer in the typical solar cells CIGS and CZTS cells [16, 17]. This may be attributed to that for the films annealed in vacuum more S vacancies lead to smaller unit cell volume and smaller lattice constants. Contrast data of grain size for the ZnS films annealed in different atmosphere is shown in Fig. 3. The grain sizes are enlarged after annealing for all the ZnS films except the one annealed in vacuum at 500°C . This indicates that annealing helps the enlargement of grain size, but for the sample annealed in vacuum at 500°C more S vacancy defects suppress the grain growth process resulting in the smallest size (28nm). At every same temperature, the grain size of the film annealed in S atmosphere is bigger than that annealed in vacuum, with the maximum of 32nm , which suggests that annealing in S atmosphere is more helpful to enlarge the grain size of ZnS films due to improvement in S vacancy defects.

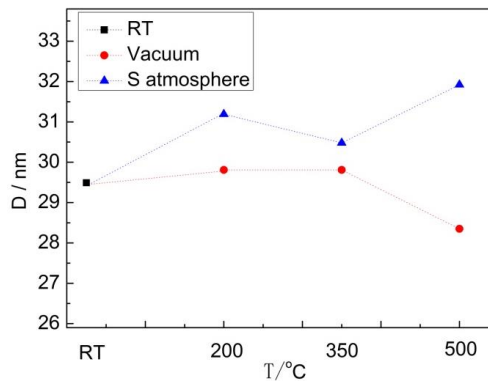


Fig. 3. The grain size of ZnS films annealed at 200°C , 350°C , 500°C in different atmosphere.

3.2. Surface morphology and atomic ratio

Fig. 4 shows SEM images of the ZnS films annealed in different atmosphere (vacuum or S atmosphere). It seems that the films are fairly good in crystalline quality, but as mentioned above in fact the films annealed at 500°C have some cracks visible to the naked eye arising from thermal stress. At the lower annealing temperature (200°C and 350°C), each film annealed in vacuum or S atmosphere has rather compact and uniform surface (Fig. 4 a, b, d, e). The surface of the film annealed at 500°C in vacuum (Fig. 4 c) is not as compact and uniform as that of the films annealed

at the lower annealing temperature, which should be due to the worse crystalline quality. As for the surface of the film annealed at 500°C in S atmosphere (Fig. 4 f), the change is not apparent. This is in agreement with the XRD data.

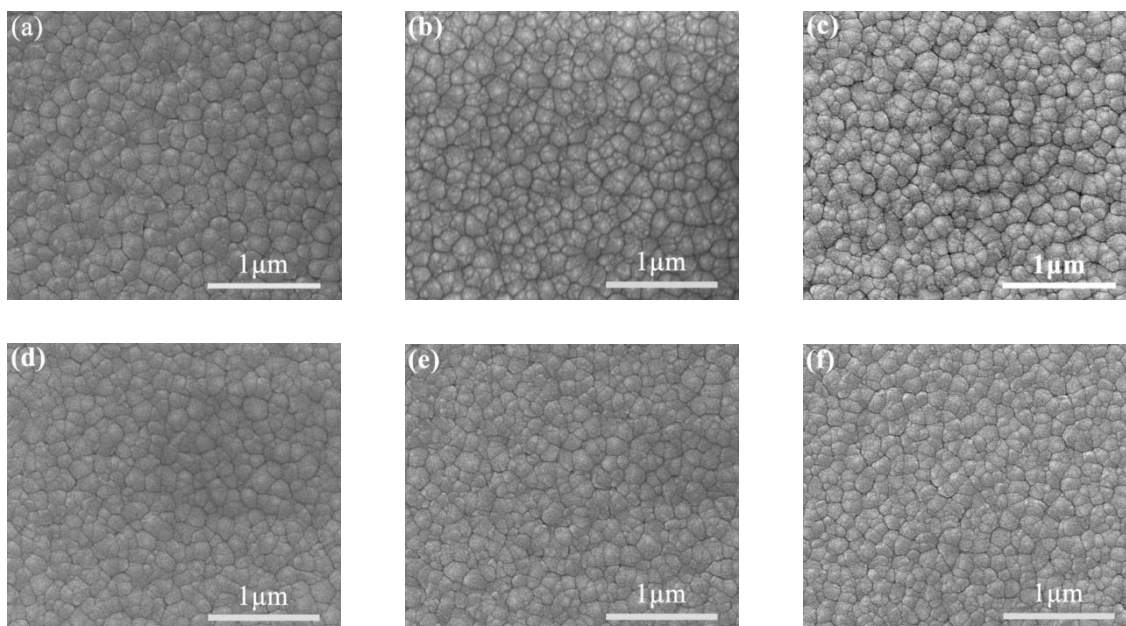


Fig. 4. The SEM images of annealed ZnS films. (a) vacuum at 200°C; (b) vacuum at 350°C; (c) vacuum at 500°C; (d) S atmosphere at 200°C; (e) S atmosphere at 350°C; (f) S atmosphere at 500°C.

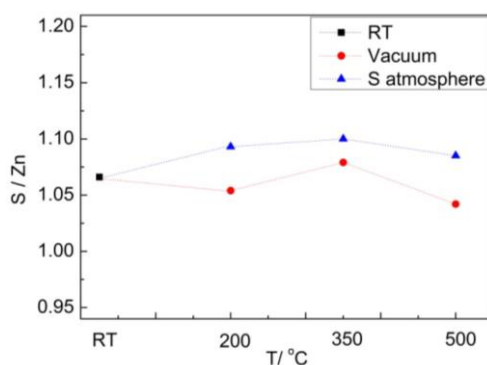


Fig. 5. The atomic ratio of ZnS films annealed at 200°C, 350°C, 500°C in different atmosphere.

The S/Zn atomic ratios of the ZnS films annealed in different atmosphere measured by EDS are shown in Fig. 5. As can be seen in Fig. 5, the S/Zn ratio of ZnS film annealed in S atmosphere is elevated comparing with that annealed in vacuum at every same annealing temperature, and the difference between them is most obvious at 500°C. The S/Zn atomic ratios of all the samples are near the stoichiometric composition, with some shift less than 10% which might be formed by all possible kinds of defects in the films such as S, Zn interstitial defects and S, Zn vacancy defects. S atmosphere annealing method mainly changes the S vacancy defects, improving S reevaporation comparing with vacuum annealing method. This improvement should be observed most obviously when at higher annealing temperature with a greater likelihood of S reevaporation, so the S/Zn ratio difference between S atmosphere annealed sample and vacuum annealed sample is the biggest at 500°C.

3.3. Optical constants

Optical constants (n , k) of the samples were obtained using ellipsometer and DeltaPsi2 software. Fig. 6 presents the refractive index (n) of the ZnS thin films annealed in different atmosphere. On the whole, all the films have rather high n values (2.03 ~ 2.31) in the visible wavelength range of 1.5-2.9eV, which is in agreement with reported reference [18]. At every same annealing temperature, the n value of the ZnS films annealed in S atmosphere is lower than that annealed in vacuum. Refractive index of films relates to packing density [19]. Maybe the different annealing atmosphere influenced the packing density of the ZnS films. The extinction coefficient (k) of the ZnS thin films can be seen in Fig. 7. All the ZnS films are transparent in visible wavelength range with k values of 0.0028 - 0.014, close to zero. This is good if ZnS is used as buffer layer in film solar cells because of more light into the absorber layer.

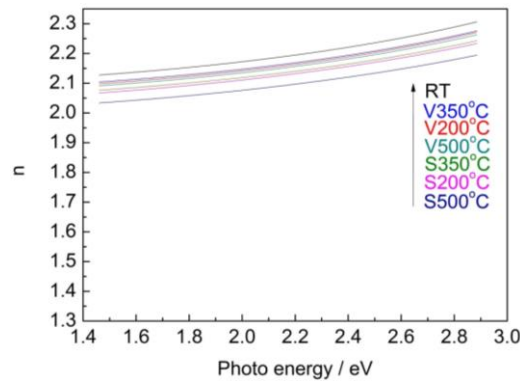


Fig. 6. The refractive index of ZnS films annealed at 200°C, 350°C, 500°C in different atmosphere. “V”: Vacuum. “S”: S atmosphere.

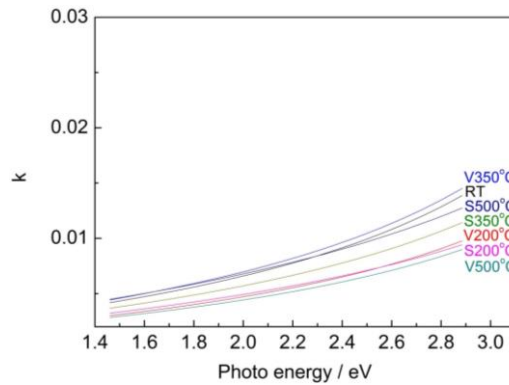


Fig. 7. The extinction coefficient of ZnS films annealed at 200°C, 350°C, 500°C in different atmosphere.

3.4. Raman spectrum

Fig. 8 depicts Raman spectra of the ZnS films annealed in different atmosphere. In Fig. 8 we can see that all the films exhibit similar Raman characteristics, one obvious peak at about 350cm^{-1} and one weaker broad peak ranging from 235cm^{-1} to 285cm^{-1} , except the film annealed in vacuum at 500°C . The former corresponds to the first-order LO Raman mode. The latter is more complex, corresponding to the combination of the first-order TO phonon Raman scattering and the second-order two-phonon Raman scattering [20, 21]. As we can see in Fig. 8, background

fluorescence emerges in the Raman spectra of all the ZnS films after annealing treatment, and the higher the annealing temperature is, the intenser the background fluorescence becomes. ZnS is fluorescent material, and its photoluminescence property may be advantageous to device performance when ZnS film is used as buffer layer in solar cells. As mentioned above, only the film annealed at 500°C in vacuum doesn't show any ZnS Raman peak, which is due to its comparatively worse crystalline quality and the intenser fluorescence background. While the film annealed at 500°C in S atmosphere exhibits the ZnS Raman peaks though also disturbed by the intenser background fluorescence, which is because of its better crystalline quality than that annealed at 500°C in vacuum by improving S vacancy defects. The Raman result also agrees with the XRD data.

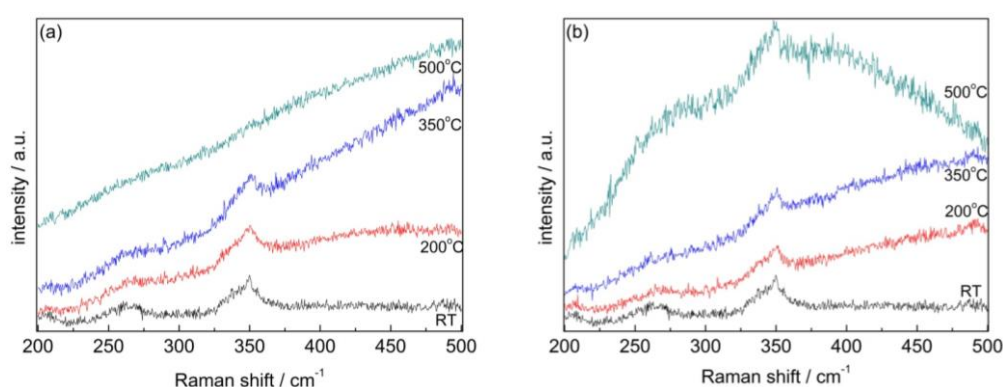


Fig. 8. The Raman spectra of ZnS films annealed at 200°C, 350°C, 500°C in different atmosphere. (a) vacuum; (b) S atmosphere.

3.5. Transmittance spectra and band gap

Fig. 9 presents the transmittance spectra of the ZnS films annealed in different atmosphere in the wavelength range from 360nm to 1000nm. The plots indicate that the samples possess good optical transparency in visible and part of near infrared wavelength range with the average transmittance minimum of 70% and the maximum of 85%.

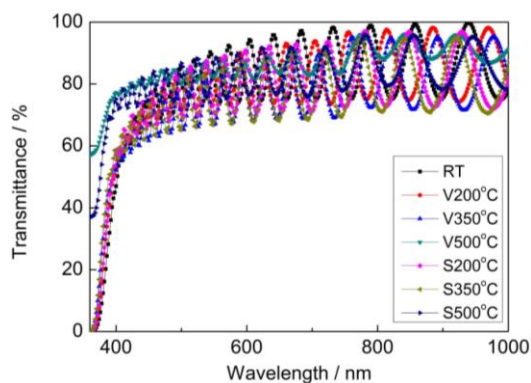


Fig. 9. The transmittance spectra of ZnS films annealed at 200°C, 350°C, 500°C in different atmosphere.

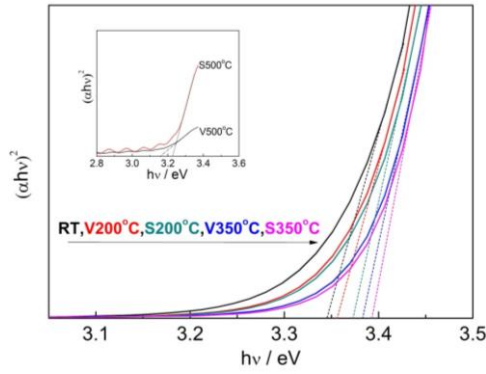


Fig. 10. The variation of the square of the product of absorption coefficient and photon energy versus photon energy for the ZnS films annealed at 200°C, 350°C, 500°C in different atmosphere. The inset is the curves of ZnS films annealed at 500°C.

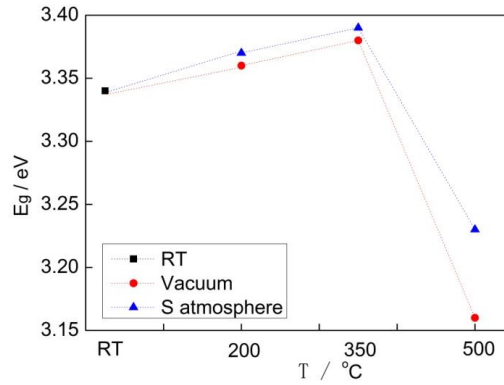


Fig. 11. The band gap of ZnS films annealed at 200°C, 350°C, 500°C in different atmosphere.

The E_g value of a semiconductor can be estimated using the Tauc formula:

$$\alpha hv = A(hv - E_g)^{n/2} \quad (4)$$

where A is a constant, α is the absorption coefficient and n is 1 for direct band gap semiconductor and 3 for indirect band gap semiconductor. ZnS is a direct band gap semiconductor, so n is 1 for it. The variation of the square of the product of absorption coefficient and photon energy $(\alpha hv)^2$ versus photon energy hv for the ZnS films annealed in different atmosphere is presented in Fig. 10 and the curves of the ZnS films annealed at 500°C are given in an inset of Fig. 10 for some significant difference from others. E_g of ZnS films can be obtained by extrapolating the straight line of the curves to the hv axis, and the E_g values are shown in Fig. 11 ranging from 3.16eV to 3.39eV. The property of wide band gap makes ZnS suitable for buffer layer of film solar cells, permitting more light especially the short wavelength light into absorber layer. Whether annealed in vacuum or in S atmosphere, the band gap of the films annealed at 500°C is not as wide as that annealed at other temperatures (200°C, 350°C), with the one annealed at 500°C in vacuum at the minimum of 3.16eV. In Fig. 11 we can see that at every same annealing temperature, the band gap of the film annealed in S atmosphere is wider than that annealed in vacuum, with the band gap difference at 500°C at the maximum of 0.07eV. Band gap of films relates to defect concentration [20], so the blue shift of the band gap for the ZnS films annealed in S atmosphere may be due to lower concentration of S vacancies than that annealed in vacuum. The band gap difference reaches the maximum at 500°C, which may be attributed to the maximum difference of

S vacancy defects concentration at the temperature between the two kinds of films annealed in different atmosphere. This is consistent with the results of EDS atomic ratio.

4. Conclusions

ZnS films were deposited on quartz glass substrates by RF magnetron sputtering, and were annealed at 200°C, 350°C, 500°C in a vacuum atmosphere and a sulfur atmosphere, respectively. This route is hopeful to achieve industrial production of ZnS films. Experimental data in this work shows that higher quality ZnS films have been obtained when annealed at 200°C, 350°C in S atmosphere than in vacuum which had dense and homogeneous surface, good crystallinity, lattice matching with absorber layer, and wide band gap.

The problems of both sulfur vacancies and thermal stress had apparent negative effects on the film quality when ZnS films were annealed at higher temperature (500°C). The thermal stress problem might be solved by using substrate with more matched thermal expansion coefficient with ZnS. Sulfur vacancies can be reduced by annealing in the sulfur atmosphere. It is estimated that better results might be obtained if the sulfur atmosphere is further strengthened in our next work.

Acknowledgements

This work was supported by the Funding for the development project of Beijing Municipal Education Commission of Science and Technology, China (Grant No.KZ201410005008) and the Natural Science Foundation of Beijing, China (Grant No. 4102014).

References

- [1] R. Zhang, B. Wang, L. Wei, X. Li, Q. Xu, S. Peng, I. Kurash, H. Qian *Vacuum* **86**, 1210 (2012).
- [2] E.M. Mkawi, K.Ibrahim, M.K.M. Ali, M.A. Farrukh, A.S. Mohamed Solar, *J. Electron. Mater.* **44**, 3380 (2015).
- [3] H. Xu, L. Wu, W. Wang, L. Zhang, J. Zhang, W. Li, L. Feng *International Journal Of Photoenergy* **2014**, 720560 (2014).
- [4] S. Ummartyotin, Y. Infahsaeng *Renew. Sust. Energ. Rev.* **55**, 17 (2016).
- [5] J. S. Cruz, D. S. Cruz, M. C. Arenas-arrocena, F. D. M. Flores, S. A. M. Hernandez *Chalcogenide. Lett.* **12**, 277 (2015).
- [6] M. Nguyen, K. Ernits, K. F. Tai, C. F. Ng, S. S. Pramana, W. A. Sasangka, S. K. Batabyal, T. Holopainen, D. Meissner, A. Neisser, L. H. Wong *Sol. Energy.* **111**, 344 (2015).
- [7] M. Buffière, S. Harel, C. Guillot-Deudon, L. Arzel, N. Barreau, J. Kessler *physica status solidi (a)* **212**, 282 (2015).
- [8] P. Chelvanathan, Y. Yusoff, F. Haque, M. Akhtaruzzaman, M.M. Alam, Z.A. Alothman, M.J. Rashid, K. Sopian, N. Amin *APPL. SURF. SCI.* **334**, 138 (2015).
- [9] F. K. Ampong, J.A.M. Awudza, R.K. Nkum, F. Boakye, P. J. Thomas, P. O'Brien *Solid. State. Sci.* **40**, 50 (2015).
- [10] S. Tec-Yam, J. Rojas, V. Rejón, A.I. Oliva *Mater. Chem. Phys.* **136**, 386 (2012).
- [11] S. Takata, T. Minami, T. Miyata, H. Nanto *J. Cryst. Growth.* **86**, 257 (1988).
- [12] M.M. Islam, S.Ishizuka, A.Yamada, K.Sakurai, S.Niki, T.Sakurai, K.Akimoto *Sol. Energ. Mat. Sol. C.* **93**, 970 (2009).
- [13] M. R. A. Bhuiyan, M. M. Alam, M. A. Momin *Turk. J. Phys.* **34**, 43 (2010).
- [14] B. R. Koo, Y. T. Oh, D. C. Shin *Journal of Advanced Engineering and Technology* **8**, 201 (2015).
- [15] J. Díaz-Reyes, R.S. Castillo-Ojeda, R. Sanchez-Espíndola, M. Galvan-Arellano,

- O. Zaca-Moran *Curr. Appl. Phys.* **15**, 103 (2015).
- [16] B. Vidhya, S. Velumani, J. A. Arenas-Alatorre, A. Morales-Acevedo, R. Asomoza, J.A. Chavez-Carvayar *Materials Science and Engineering B* **174**, 216 (2010).
- [17] S. Schorr, H. Hoebler, M. Tovar *Eur. J. Mineral.* **19**, 65 (2007).
- [18] D. Prakasha, A.M.Aboraiab, M.El-Hagaryc, E.R.Shaabanb, K.D.Verma *Ceram. Int.* **42**, 2676 (2016).
- [19] T. E. Varitimos, R. W. Tustison *Thin Solid Films* **151**, 27 (1987).
- [20] Y. C. Cheng, C. Q. Jin, F. Gao, X. L. Wu, W. Zhong, S. H. Li, P. K. Chu *J. Appl. Phys.* **106**, 123505 (2009).
- [21] J. Kennedy, P.P.Murmu, P.S.Gupta, D.A.Carder, S.V.Chong, J. Leveneur, S.Rubanov *Mat. Sci. Semicon. Proc.* **26**, 561 (2014).